AGU PUBLICATIONS

Space Weather

RESEARCH ARTICLE
10.1002/2015SW001345

Spacecraft surface charging within geosynchronous orbit observed by the Van Allen Probes

Lois K. Sarno-Smith[1], Brian A. Larsen[2], Ruth M. Skoug[2], Michael W. Liemohn[1], Aaron Breneman[3], John R. Wygant[3], and Michelle F. Thomsen[4]

[1]Department of Climate and Space Engineering, University of Michigan, Ann Arbor, Michigan, USA, [2]Los Alamos National Laboratory, Los Alamos, New Mexico, USA, [3]School of Physics and Astronomy, University of Minnesota, Minneapolis, Minnesota, USA, [4]Planetary Science Institute, Tucson, Arizona, USA

Key Points:
- Statistical analysis of Van Allen Probes spacecraft charging
- Intense negative charging occurs in sunlight
- Electron Pressure, temperature, and fluxes affect charging occurrence and intensity

Correspondence to:
L. K. Sarno-Smith,
loisks@umich.edu

Citation:
Sarno-Smith, L. K., B. A. Larsen, R. M. Skoug, M. W. Liemohn, A. Breneman, J. R. Wygant, and M. F. Thomsen (2016), Spacecraft surface charging within geosynchronous orbit observed by the Van Allen Probes, *Space Weather*, *14*, 151–164, doi:10.1002/2015SW001345.

Received 20 NOV 2015
Accepted 3 FEB 2016
Accepted article online 6 FEB 2016
Published online 27 FEB 2016

Abstract Using the Helium Oxygen Proton Electron (HOPE) and Electric Field and Waves (EFW) instruments from the Van Allen Probes, we explored the relationship between electron energy fluxes in the eV and keV ranges and spacecraft surface charging. We present statistical results on spacecraft charging within geosynchronous orbit by L and MLT. An algorithm to extract the H^+ charging line in the HOPE instrument data was developed to better explore intense charging events. Also, this study explored how spacecraft potential relates to electron number density, electron pressure, electron temperature, thermal electron current, and low-energy ion density between 1 and 210 eV. It is demonstrated that it is imperative to use both EFW potential measurements and the HOPE instrument ion charging line for examining times of extreme spacecraft charging of the Van Allen Probes. The results of this study show that elevated electron energy fluxes and high-electron pressures are present during times of spacecraft charging but these same conditions may also occur during noncharging times. We also show noneclipse significant negative charging events on the Van Allen Probes.

1. Introduction

Spacecraft surface charging is a serious concern for satellites near geosynchronous orbit. Spacecraft anomalies have been linked to spacecraft surface charging events, particularly in the postmidnight sector where there are increased electron fluxes [e.g., *Rosen*, 1976; *Grard et al.*, 1983]. Spacecraft charging not only affects plasma measurements but also the operations of telecommunication satellites and solar panels [e.g., *Lanzerotti et al.*, 1998; *Katz et al.*, 1998; *Lanzerotti*, 2001; *Choi et al.*, 2011; *Mazur and O'Brien*, 2012]. Our ability to prevent and mitigate spacecraft charging relies on our understanding of spacecraft charging and what causes it.

One of the first reported instances of spacecraft charging was a rocket study where the authors discussed how measured ion peaks from the radio frequency mass spectrometer onboard could be explained by a −20 V surface potential [*Johnson and Meadows*, 1955]. Extreme spacecraft charging conditions on the order of −10,000 V were first recorded by geosynchronous satellites ATS 5 and ATS 6 [*DeForest*, 1972, 1973]. ATS 5 and ATS 6 were largely nonconducting satellites, as was the Spacecraft Charging at High Altitude (SCATHA) satellite which also observed extreme charging [*Olsen*, 1981; *Craven et al.*, 1987]. Spacecraft surface charging at geosynchronous orbit has been studied extensively, but conclusions have been varied. Extreme negative spacecraft charging occurs primarily when satellites enter the plasma sheet and are bathed in hot electrons in low density plasma [*Garrett*, 1981]. During intense electron flux periods, the electrons generate a strong negative current, overtaking the positive photoemission current on the spacecraft surface and resulting in a net negative current on the spacecraft. One study found that surface charging is so sensitive to location that nearby satellites cannot be used to estimate or predict another spacecraft's surface charging [*Koons et al.*, 2006]. The variability in both satellite construction and situational evidence has made it difficult to quantify spacecraft charging intensity and the factors that cause spacecraft charging.

It is known that electron fluxes are linked to negative spacecraft surface charging. However, there is still much debate as to exactly how the electron fluxes cause spacecraft charging. Measurements from SCATHA suggested spacecraft charging was produced by the 3 to 30 keV population [*Reagan et al.*, 1981]. Yet another study found that spacecraft charging intensity was caused by the electron population above 30 keV

[*Mullen et al.*, 1986]. Another study using ATS 6 and SCATHA measurements showed that once a certain threshold of 10 to 20 keV fluxes was reached, spacecraft charging would occur [*Olsen*, 1983]. There is also considerable evidence that spacecraft potential is a function of ambient electron temperature around the spacecraft [*Rubin et al.*, 1980; *Laframboise and Kamitsuma*, 1983; *Harris*, 2003].

With data from the Los Alamos National Laboratory geosynchronous (LANL-GEO) satellite program, more studies defining a critical temperature or threshold flux emerged. One such study concluded that depending on the satellite, charging will only occur when average electron temperatures near the satellite are at least between 400 and 3000 eV [*Lai and Della-Rose*, 2001]. Specifically, for the LANL-GEO satellites, which were non-conducting satellites, a critical electron temperature between 1 and 2 keV would result in extreme charging events with spacecraft potential below −200 V [*Lai and Tautz*, 2006]. A later study found that once a critical threshold of electron energy fluxes within the energy range of 5–10 keV has been satisfied, charging will occur and then the degree of charging was determined by the electron temperature [*Thomsen et al.*, 2013].

The Van Allen Probes satellites, or the Radiation Belt Storm Probes, offer us another way to analyze spacecraft charging. A pair of twin probes launched in 2012 into an approximately 9 h elliptical orbit, the Van Allen Probes contain two instruments which provide the opportunity to study spacecraft charging on a conducting spacecraft within geosynchronous orbit [*Mauk et al.*, 2014; *Kirby et al.*, 2014].

The first approach used the Helium Oxygen Proton Electron (HOPE) [*Funsten et al.*, 2014] mass spectrometer to extract the ion charging line in the proton spectra, similar to the method used in the analysis of LANL GEO data. The HOPE instrument consists of an electrostatic analyzer followed by channel electron multiplier (CEM)-based time-of-flight (TOF) pixels that measures 1 eV to 50 keV Helium, Oxygen, and Hydrogen ions along with 15 eV–50 keV electrons. Angular measurements are derived using five polar pixels (0, ±36°, ±72°) coplanar with the spacecraft spin axis, and up to 16 azimuthal bins are acquired for each polar pixel over time as the spacecraft spins. Ions and electrons are measured on alternating spins. Ion species are determined onboard the spacecraft by the energy dependent TOF bin in which the count falls.

The second method used the Electric Fields and Waves (EFW) instrument [*Wygant et al.*, 2014], which utilized two orthogonal booms in the spin plane with 100 m tip-to-tip separation to measure potential across each of the Van Allen Probes satellites, similar to other scientific double-probe spacecraft such as Polar [*Harvey et al.*, 1995]. The EFW instrument includes three pairs of sensors deployed at the tips of oppositely directed booms. The spacecraft potential is calculated on the ground by averaging probe potentials from sensors on opposite sides of the spacecraft in the spin plane. Summing and averaging removes the differential electric signal from convection, waves, and other ambient plasma processes, leaving the potential of the spacecraft body relative to the ambient plasma.

The EFW sensor is a conducting metal sphere of radius 4 cm coated with DAG 213 in order to minimize work function variations over the sphere. High-input impedance preamplifiers are located in the spheres to limit "voltage divider effects" in coupling to the ambient plasma sheath, which can have a large source impedance in a low density plasma. The spherical sensor is current biased with a constant bias current which is controlled by the EFW CPU and adjusted to balance the photoemission from the sphere. More specifically, the sensor bias current value is adjusted to have the opposite sign of the photocurrent from the sphere and at about 20–50% of its magnitude. This operating point is determined by periodic bias sweeps that involve stepping the bias current and measuring the output voltage of the sensor.

Sections of the boom near the sphere are voltage biased at constant positive (1–3 V) potential relative to the sphere potential in order to limit spurious photo currents flowing between the sensor and the nearby boom elements. The power supply limits for the sensor preamplifier are ±200 V. This corresponds to the largest signal that can be measured by the preamplifier. Thus, if the spacecraft charges to more than 200 V, the preamplifiers "saturate." In order to limit differential charging of the spacecraft, the spacecraft bus is constructed from conductive materials. The solar panels include Indium Tin Oxide (ITO) coated cover glasses. The thermal blankets are similarly coated ITO coatings. All conductive surfaces including the backs of the solar panels on the spacecraft are conductively tied together to limit charging between the sunlit and nonilluminated sections of the spacecraft. The purpose of the conductivity specification for spacecraft surfaces was to insure that all surfaces of the spacecraft be conductive such that no differential charging from any two regions on the spacecraft bus with areas larger than approximately 1 cm^2 could exceed 1 V when in orbit. This conductivity specification is designed to limit the differential charging believed to play an important role near geosynchronous orbit.

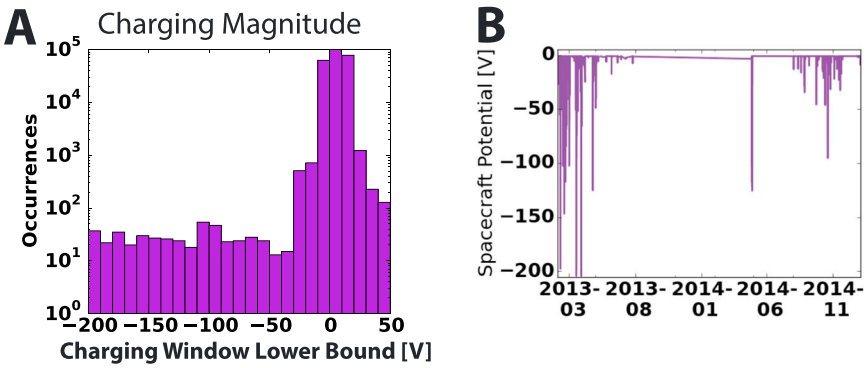

Figure 1. (a) The number of EFW charging events from February 2013 to April 2015 over the range of −200 V to 50 V in 10 V windows. The *x* axis labels give the lower bound for each window. An occurrence is defined a single measurement by EFW over an 11 s window. (b) The negative spacecraft potential recorded by EFW over the February 2013 to April 2015 time period.

Each method has strengths and weaknesses. The HOPE ion extraction method can only capture times of negative spacecraft charging, and it performs best when charging is below −50 V. The HOPE ion extraction algorithm we use requires that EFW identifies periods of negative charging and then looks for the ion line. On the other hand, the EFW probe potential method measures spacecraft charging at all times both positive and negative, but it saturates due to voltage limitations at ±200 V of negative spacecraft potential. This study demonstrates that EFW tends to underestimate times of intense charging lower than −50 V.

EFW is additionally limited since it cannot make reliable spacecraft potential measurements, while in Earth's shadow because the photocurrents necessary to produce a stable potential reference for the probes are not present [*Wygant et al.*, 2014]. The electric field probes are current biased to produce a stable voltage reference. In a low density plasma during times of solar illumination, the two dominant currents are (1) photoemission and (2) a fixed bias current from the sensor that is controlled by the EFW microprocessor. When these two currents are balanced properly, the sensor floats at a nearly constant potential within 1–2 V of the plasma potential at infinity. When the spacecraft is in Earth's shadow, there is no photoemission current. The current balance lies between the EFW controlled bias current and plasma currents, which can result in large sensor floating potentials and large DC sheath impedances. Thus, EFW and other double-probe electric field experiments are not designed to provide accurate electric field measurements during eclipse periods in low density plasmas.

In this study, surface charging was statistically analyzed on the Van Allen Probes satellites as a function of L and magnetic local time (MLT). The relationship between surface charging and electron pressure, electron temperature, thermal electron current, low-energy ambient ion density, and electron density was examined. A comparison between the two methods of calculating spacecraft charging, using the HOPE instrument H^+ spectra and EFW potential measurements, was performed. The relationship between thermal current and electron energy fluxes was also examined in this study.

2. Observations From EFW

Figure 1 shows the distribution of charging occurrences and magnitudes in the Van Allen Probes EFW measurements from February 2013 to April 2015. Combining EFW data from both Van Allen Probes A and B satellites, Figure 1a shows that each satellite usually charged within ±10 V during this time period. Charging events less than −50 V occurred 4 orders of magnitude less often than ±10 V charging times. Figure 1b highlights that most of the negative charging events throughout the mission occurred in the first 4 months of 2013 and from August to December of 2014, when the apogee of the satellites was in the postmidnight sector.

Using times of spacecraft charging between February of 2013 and April of 2015, spacecraft potential from the EFW instrument on both Van Allen Probes A and B was binned by L and MLT. These spacecraft potential measurements were binned by 0.25 L and 0.5 MLT and put into four charging windows: <−10 V, −10 V to 0 V, 0 V to 10 V, and >10 V. The Olson-Pfitzer 77 model is used to calculate L [*Olson and Pfitzer*, 1977].

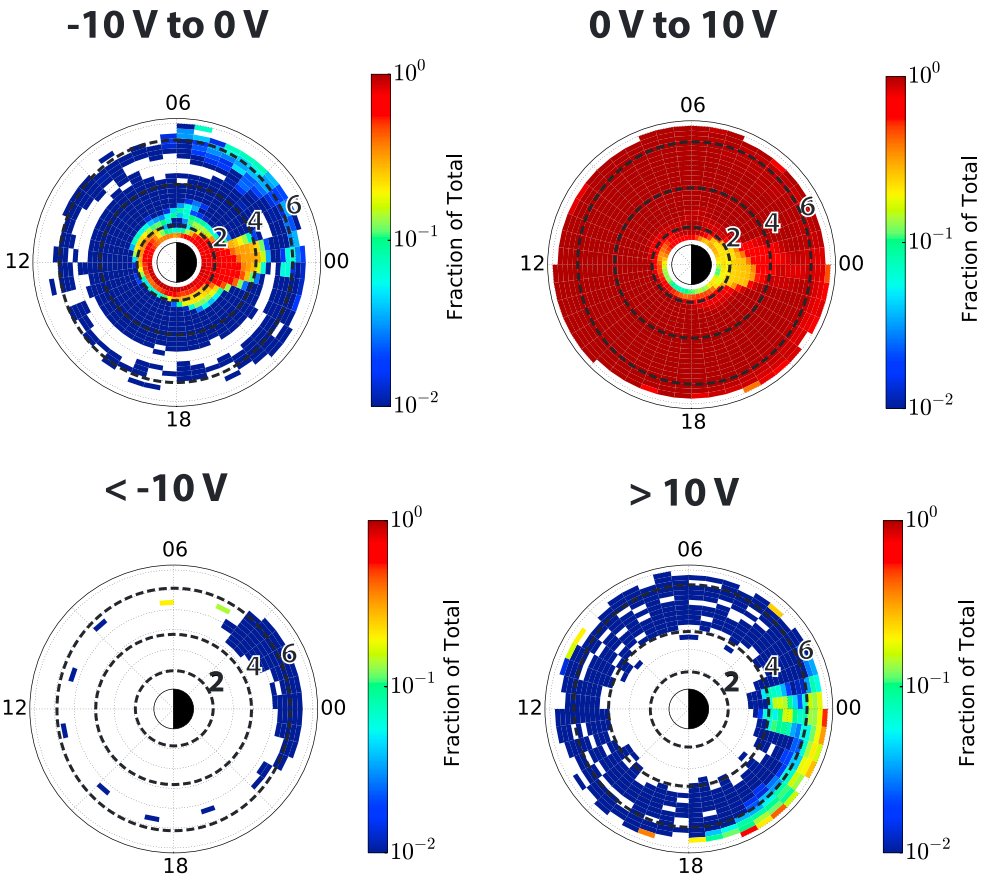

Figure 2. EFW Van Allen Probes A and B spacecraft potential categorized as 0 to −10 V, 0 to 10 V, <−10 V, and >10 V and binned by 0.5 MLT and 0.25 L from February 2013 to April 2015. The fraction reflects the number of 11 s measurements in each charging window and 0.5 MLT/0.25 L bin compared to all the measurements from that MLT and L. The reddish background in the 0 to 10 V category is because of the vast majority of measurements occur in this charging window.

Figure 2 shows normalized spacecraft potential as a function of MLT and L for each level of charging. The total number of occurrences is used to normalize the results in each L/MLT bin. Most instances of −10 V to 0 V charging occurred at L < 3 at all local times. Times when the spacecraft was in Earth's shadow are identified by nearly 100% likelihood of slight negative charging (−10 V to 0 V). This is because solar driven photoemission is curtailed from lack of sunlight, and as a consequence, the spacecraft charges slightly negative. Some charging events also occurred in the postmidnight sector at L > 4 in this charging window. The 0 V to 10 V charging window encompasses most of the data from the mission, with small gaps across the nightside, pre-evening sectors, and in Earth's shadow. Only a few <−10 V events are observed, all at L > 4. Most of the events occurred in the postmidnight sector, but some events also occurred at dawn and in the premidnight sectors. This is agrees with the results observed by ATS-6 [*Reasoner et al.*, 1976]. For >10 V of positive charging, the majority of events occur at either midnight or premidnight at L > 3.

Figure 3 highlights times of negative charging on the Van Allen Probes when the spacecraft was not in eclipse. Charging occurrences from both Van Allen Probes A and Van Allen Probes B were included in Figure 3. In this situation, the thermal electron current spikes due to the presence of hot electrons and exceeds the photoemission current which usually keeps the spacecraft slightly positive. These times of negative charging in sunlight present a unique situation. Extreme care was taken on the Van Allen Probes satellites to ensure a conducting spacecraft, and previous studies have shown, based on model results, that significant negative spacecraft charging should not occur in sunlight on a conducting spacecraft [*Davis et al.*, 2012; *Kirby et al.*, 2014]. In particular, we see from Figure 3 in the postmidnight sector at L > 4, there are a large number of negative spacecraft charging events, where hot electrons begin to gradient curvature drift eastward as they enter from the plasma sheet.

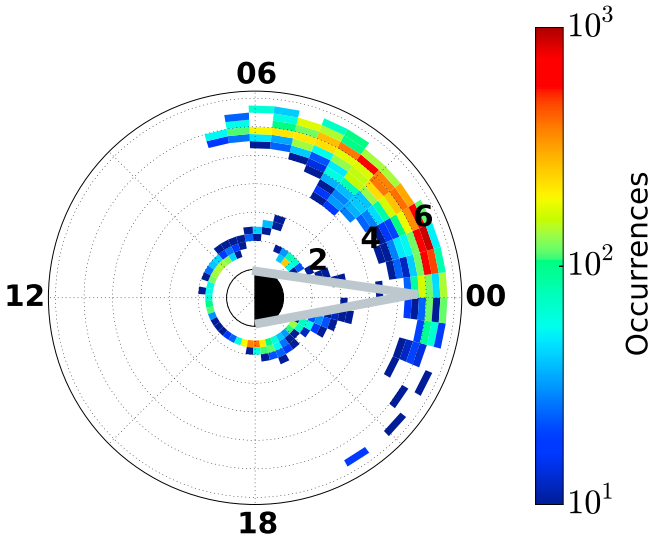

Figure 3. Times of negative charging measured by both Van Allen Probes A and B EFW instruments outside of eclipse periods. The spacecraft charge was binned by 0.5 MLT and 0.25 L from February 2013 to April 2015. The silver line shows where we would expect eclipse to be based on average Van Allen Probes satellite orbital parameters.

We examine the 0–10 V charging window more closely by further dividing this window into 1 V bins; Figure 4 shows selected bins. Most observations at $L < 4$ show 0–1 V charging. By 2–3 V positive potential, there are almost no events at $L < 3$. Instead, there is a stronger likelihood of these positive events to occur in the dusk sector after MLT = 18 between $4 < L < 6$. In the 4–5 V window, charging is most likely to occur at dawn with MLT = 6 just inside of L = 5. There are only a few events in the 8–9 V window, and they most often occur in the premidnight sector at $L > 5$. Positive charging appears to be related to the average plasmapause boundary at L = 4. Minimal positive spacecraft charging of 0 to 1 V occurs almost 100% of the time within L = 4. More intense positive charging events with charging >2 V occur outside of L = 4.

3. Spacecraft Potential From HOPE Instrument Ion Line Extraction

Two major constraints of the EFW potential measurements are that the instrument saturates at −200 V due to voltage limitations and EFW potential measurements are unreliable during eclipse times when the satellite is in Earth's shadow. However, we can still get a measurement for spacecraft charging during EFW saturation times. We developed an algorithm to extract the charging line from the HOPE instrument H^+ spectra. The charging line occurs when the spacecraft charges negative, and all ions are accelerated by the spacecraft potential as they approach the detector. An ion with an energy of 3 eV would accelerate to 103 eV if the charging on the spacecraft is −100 V. The bulk ion acceleration manifests in the counts spectra as a ribbon of high counts and appears at the level of charging. For −100 V of charging, there would be a line of high counts in the 100 eV measurement bin. In this situation, the detector should observe no ions below 100 eV.

However, at times of significant charging on the Van Allen Probes, there were still counts in the lower energy portion of the spectrum. Therefore, we first employed a base level subtraction technique. To obtain an average base count level, we binned the number of proton counts from 1 eV to 50 keV in the HOPE instrument by 0.1 L between February 2013 and April 2015. Then, for each L and energy bin, the base level counts were defined as the median counts in that bin. The base level counts were highest at low L and at low energies, but above 100 eV were low and usually close to zero.

We subtracted the base count number from each energy bin at each time interval in the HOPE instrument data between February 2013 and April 2015. To identify the charging line was, we looked at times with $L > 5$ and periods where EFW showed negative charging. Based on Figure 2, the $L > 5$ assumption is reasonable for times of intense negative charging. During times of charging, the subtracted number of counts was typically negative below the charging line because of the base level subtraction. We then found the three lowest-energy points with nonzero subtracted counts in each energy spectrum and determined if these points showed a

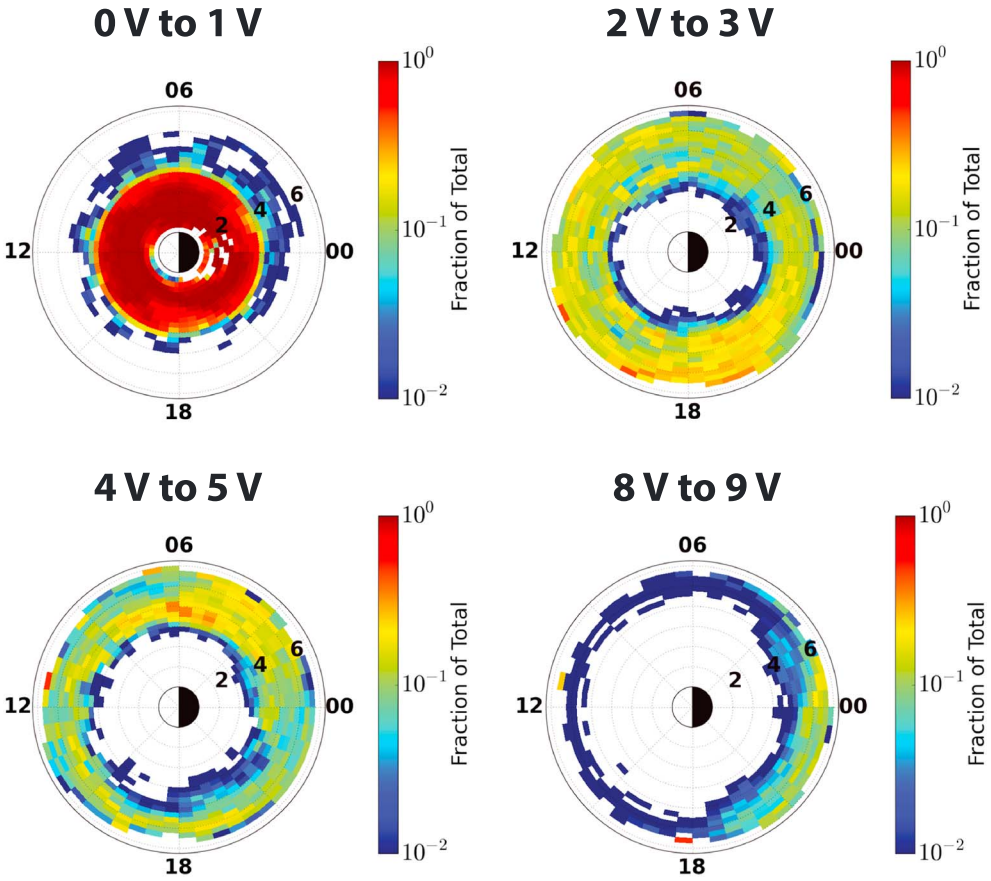

Figure 4. Van Allen Probes A and B EFW positive spacecraft potential in selected 1 V charging windows binned by 0.5 MLT and 0.25 L from February 2013 to April 2015 in the same format as Figure 2.

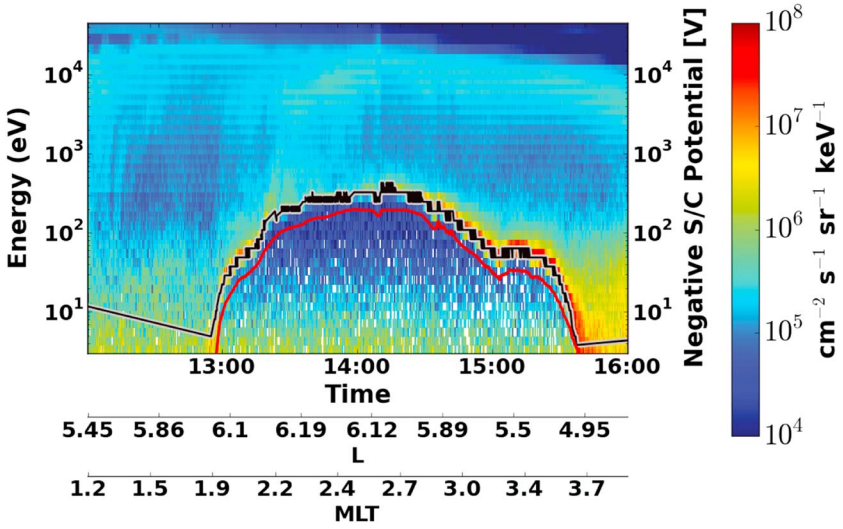

Figure 5. Spacecraft charging on 8 February 2013 from Van Allen Probes A, with the red line as the negative EFW spacecraft potential and the black silver edged line as the HOPE instrument charging line from 12:00 to 16:00 UT. The silver line width is the HOPE energy channel width in eV measuring the H^+ charging line. The spectrogram shows HOPE H^+ differential number flux over the same time period. The satellite was not in eclipse during this charging event.

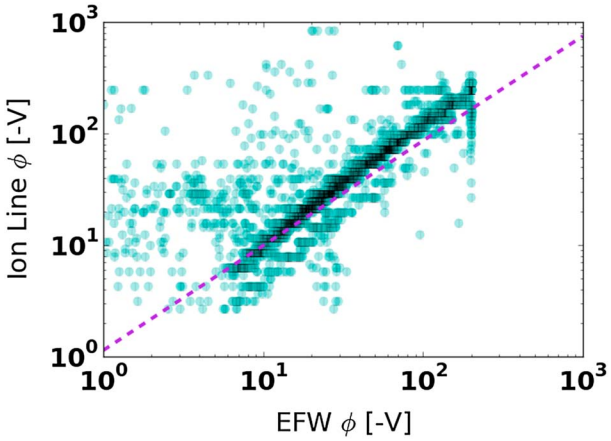

Figure 6. The negative spacecraft potential measured by EFW and extracted from the HOPE H^+ line at the same times from February 2013 to April 2015. The diameter of each point is the width of the HOPE energy channel bin (15% of the measured energy) corresponding to that measurement. The purple line is the exponential fit for scatter points within one standard deviation of where EFW ϕ = HOPE ϕ.

significant gradient in count rate. If the difference of the first and third nonzero counts was greater than 10, then we concluded that there was a charging line and identified the level of surface charging as the lowest energy with nonzero counts. The minimum gradient of 10 counts worked well at capturing times of high spacecraft charging and identifying the ribbon of accelerated ions. A higher threshold for the gradient excluded low charging events, and a lower threshold made it impossible to distinguish between small fluctuations at midenergies and times of spacecraft charging. It was necessary to use the gradient method to separate charging times from low count times and events where there were high-flux levels at higher energies.

Figure 5 shows an example of the results of our algorithm. Figure 5 shows the H^+ differential number flux spectrogram for 8 February 2013 between 12:00 and 16:00 UT. This day had a significant charging event where the spacecraft potential reached −198 V according to EFW data and −430 V according to the HOPE ion charging line. There is an uncertainty of 67.8 V on the HOPE ion charging line based on the width of the HOPE energy channel at 430 eV, and this is represented in Figure 5 by the width of the silver line. The width of the HOPE energy channels is 15% of the label for that energy channel. The EFW potential probes saturate during the charging event because the spacecraft charge was less than −200 V; thus, EFW was unable to accurately determine the charging magnitude. The charging line is clear in the flux spectrogram, and the HOPE instrument ion line extraction algorithm matches this line well.

Figure 6 compares the magnitude of charging measured by EFW and determined by the HOPE extraction method at times when both had measurements. The diameter of each point gives the width of the HOPE ion line energy channel. The blue dotted line shows the exponential fit of scatter points within one standard deviation of where EFW = HOPE data. For an exponential fit $y = Ae^B$, where A was 1.14 and B was 0 .94, confirming that HOPE measures higher potentials. In Figure 6, we can observe that the HOPE extracted ion line measures a higher negative spacecraft potential than EFW particularly during intense charging events, even with error bars taken into account. This is supported by the exponential fit having a slope > 1.

Of the 3284 1 min averaged points with both EFW and HOPE charging measurements, the HOPE potential was larger in 2221 instances. Over all times, EFW potentials were lower than HOPE potentials by a median value of 5.6 V, and a mean difference of 11.2 V. Much of this skew was due to EFW spacecraft potential measurements saturating at −200 V so the instrument was unable to capture times of extreme spacecraft charging. However, even at times of charging below −200 V, EFW tended to underestimate the level of charging. The percentage difference shows that the HOPE potential is typically 25% greater than the EFW potential, with a median difference of 17% over the mission.

It should also be noted that the uncertainty of the spacecraft potential measurement by EFW is on the order of several volts when the probes provide a stable reference to plasma potential at infinity and when spacecraft potential is less than ±200 V. The 200 V limitations is from EFW sensor power supply limits. Further, spacecraft potential may extend over larger distances than the 50 m boom length; consequently, the booms may not measure the full value of the spacecraft potential. The limits on this error are based on spacecraft potential measured by the shorter 7 m boom on the axis plane and scaled to the measured value from the 50 m booms.

In order to obtain the best possible depiction of spacecraft charging, it is necessary to use both methods. The extraction of the charging line in the HOPE instrument ion spectra is not a stand alone method, and it is best used by identifying periods of charging and comparing directly with EFW. However, EFW has been shown to underestimate spacecraft potential, saturate at −200 V of charging, and is unable to make spacecraft potential

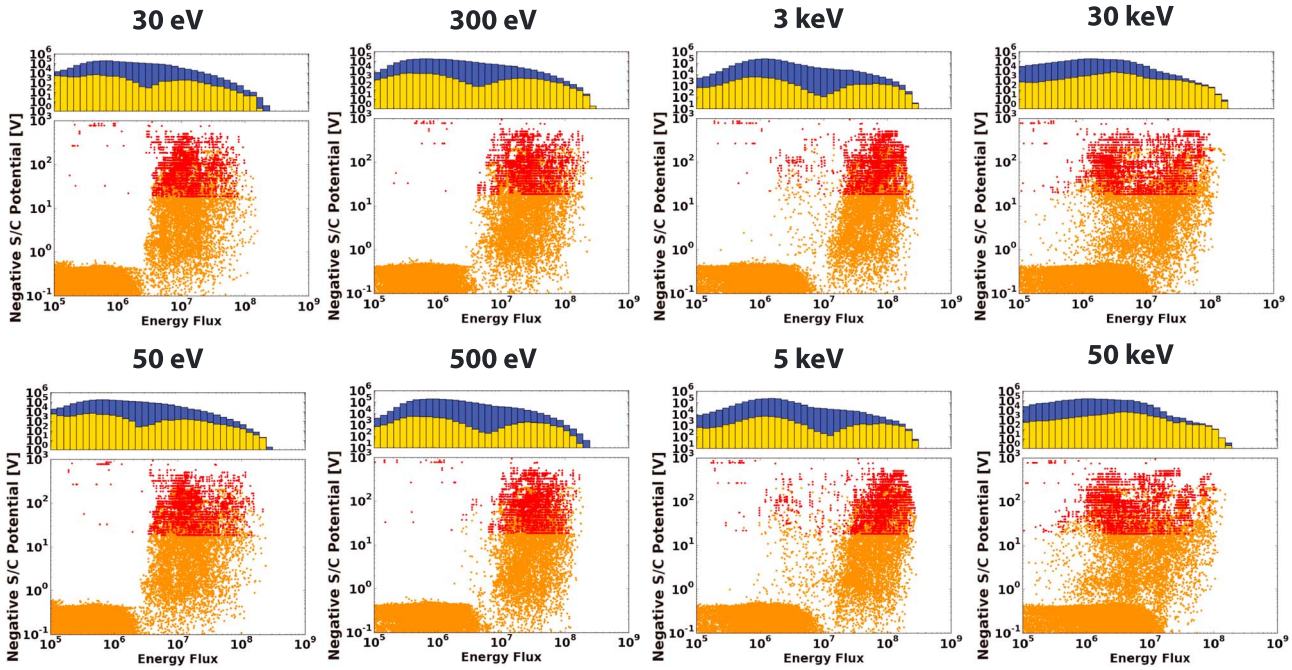

Figure 7. The negative spacecraft potential measured by EFW (orange) and HOPE (red) as a function of the electron energy flux (keV cm^{-2} s^{-1} sr^{-1} keV^{-1}) measured by the HOPE instrument. All times of negative charging from both Van Allen Probes from February 2013 to April 2015 are included. (top column) The occurrence histograms of electron energy flux measurements throughout the mission (blue) and negative charging times (yellow).

measurements during eclipse. So for certain events where there is extreme charging, using the charging line extraction technique from the HOPE instrument H^+ spectra is necessary. Coupled together, we can get a good picture of the degree of charging and when it is occurring.

4. Connection Between keV Electron Energy Fluxes and Charging

Previous studies have shown a connection between keV electron energy fluxes and spacecraft surface charging. These studies found that severe charging events all had keV electron energy flux levels above a certain threshold [*Reagan et al.*, 1981; *Olsen*, 1983; *Thomsen et al.*, 2013]. Here we repeat this study with the Van Allen Probes. Both EFW and HOPE spacecraft negative potential measurements were compared with HOPE electron energy flux measurements from February 2013 to April 2015. The data sets were averaged over 1 min intervals, and we examined times when both EFW and HOPE spacecraft potential measurements were present.

Figure 7 shows the magnitude of negative charging measured by EFW and extracted HOPE instrument ion spectra compared to the HOPE energy fluxes at 30 eV, 50 eV, 300 eV, 500 eV, 3 keV, 5 keV, 30 keV, and 50 keV energies. The orange points are the EFW spacecraft potential measurements, which saturate at 200 V. The red points are the HOPE instrument ion charging line extracted results above 10 V of negative surface charging over the same time period. Charging derived using the HOPE spectra reaches 1000 V at times.

Previous studies employed a similar method and found a distinct cutoff where a certain threshold of keV electron energy fluxes was required for large negative charging [*Reagan et al.*, 1981; *Olsen*, 1983; *Thomsen et al.*, 2013]. In both the EFW and the HOPE data, we see such a threshold in keV electron energy flux. This cut off also occurs for lower energy fluxes, extending from 1 eV to 5 keV. We define a threshold at 3×10^7 keV cm^{-2} s^{-1} sr^{-1} keV^{-1} in the 3 keV energy channel. Charging occurred at all electron energy flux levels between 10^6 and 10^9 keV cm^{-2} s^{-1} sr^{-1} keV^{-1} for all electron energy channels measured by the HOPE instrument. The results in Figure 7 confirm that there is a keV electron energy flux threshold that must be satisfied for the most intense negative spacecraft charging to occur and this threshold also occurs in <5 keV energy channels. It should be noted that there are a few occurrences of spacecraft charging during low keV electron energy fluxes.

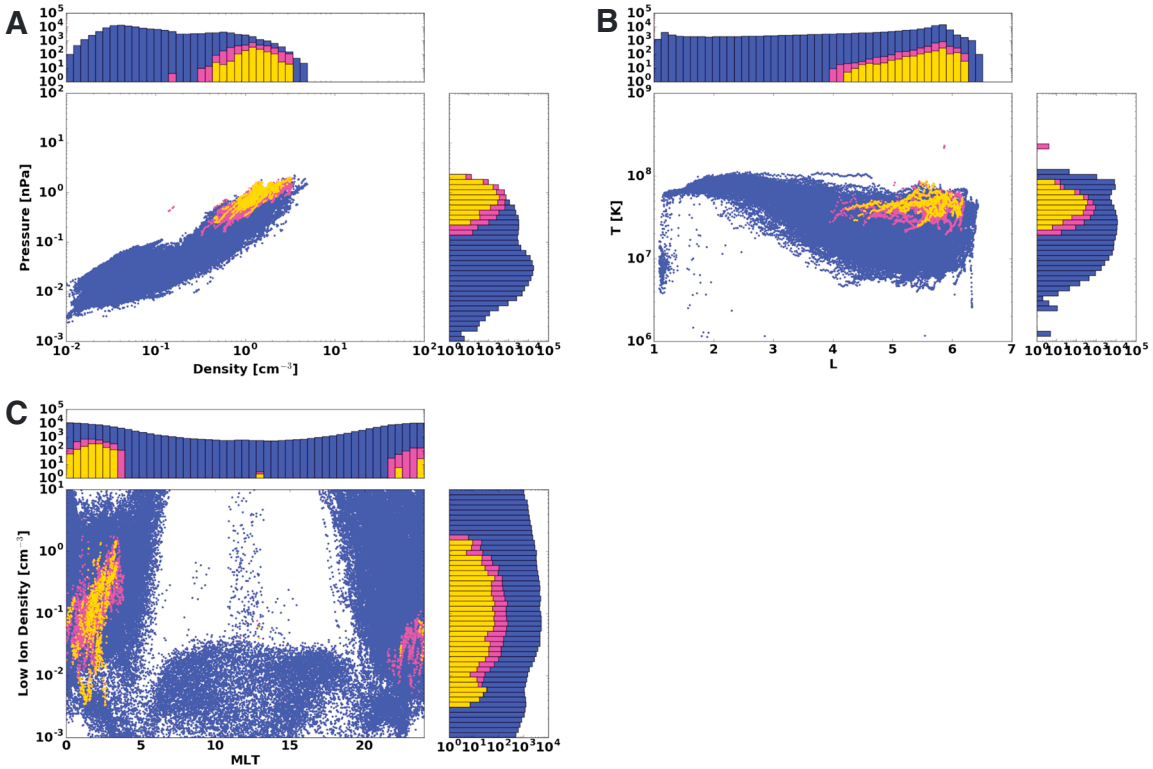

Figure 8. Resampled EFW spacecraft potential values, the HOPE instrument electron temperature (T_e), electron density (n_e), spacecraft potential corrected low-energy ion density (n_i), electron pressure (p_e), and the ephemeris MLT and L parameters from February 2013 to June 2013. (a) n_e compared to p_e. (b) L compared to T_e. (c) Low-energy ion density compared to MLT. The gold represents charging less than −25 V, the magenta represents charging less than −1 V, and blue represents charging above −1 V. The side panels represent the number of points contained within each interval.

5. Spacecraft Charging Versus Other Parameters

We examined the relationship between spacecraft charging and magnetospheric conditions, including electron temperature, electron pressure, electron density, and low-energy ion density. According to other studies, once the electron keV threshold flux at the spacecraft has been met, the overall electron temperature then determined the intensity of surface charging [*Thomsen et al.*, 2013]. We averaged all data to a 1 m cadence and included only measurements from February to June 2013, where the majority of intense charging events occurred, as can be seen in Figure 1. The electron pressure, electron density, and electron parallel and perpendicular temperatures were calculated over the 200 eV to 50 keV range; it is important to note that these parameters were not corrected for spacecraft potential and are partial moments of the quantities they represent. During significant charging, these quantities are less accurate, which adds uncertainty to our following examination of the quantities in regards to charging. The low-energy ion density was calculated between 1 and 210 eV using *Sarno-Smith et al.* [2015],

$$n_{H^+} = \sum_i 4\pi \frac{1}{\sqrt{\frac{2E_i}{m_{H^+}}}} F_{H^+} \Delta E_i, \tag{1}$$

where F_{H^+} is the H^+ differential energy flux (keV cm^{-2} s^{-1} sr^{-1} keV^{-1}). E_i is the measured energy of each energy channel of the HOPE instrument data, beginning with the 1 eV energy channel and ending with the approximately 210 eV energy channel. ΔE_i represents the range of each energy channel. The m_{H^+} and n_{H^+} notations are the H^+ mass and number density. The i in this summation represents the energy channels between 1 eV and 210 eV. We did account for spacecraft potential in the calculation of these partial densities, adjusting flux energy appropriately. During times of more than 200 V of negative charging, the low-energy ion density should be approximately 0 due to the acceleration of the ions, so some caution should be taken in the interpretation of the low-energy ion density results.

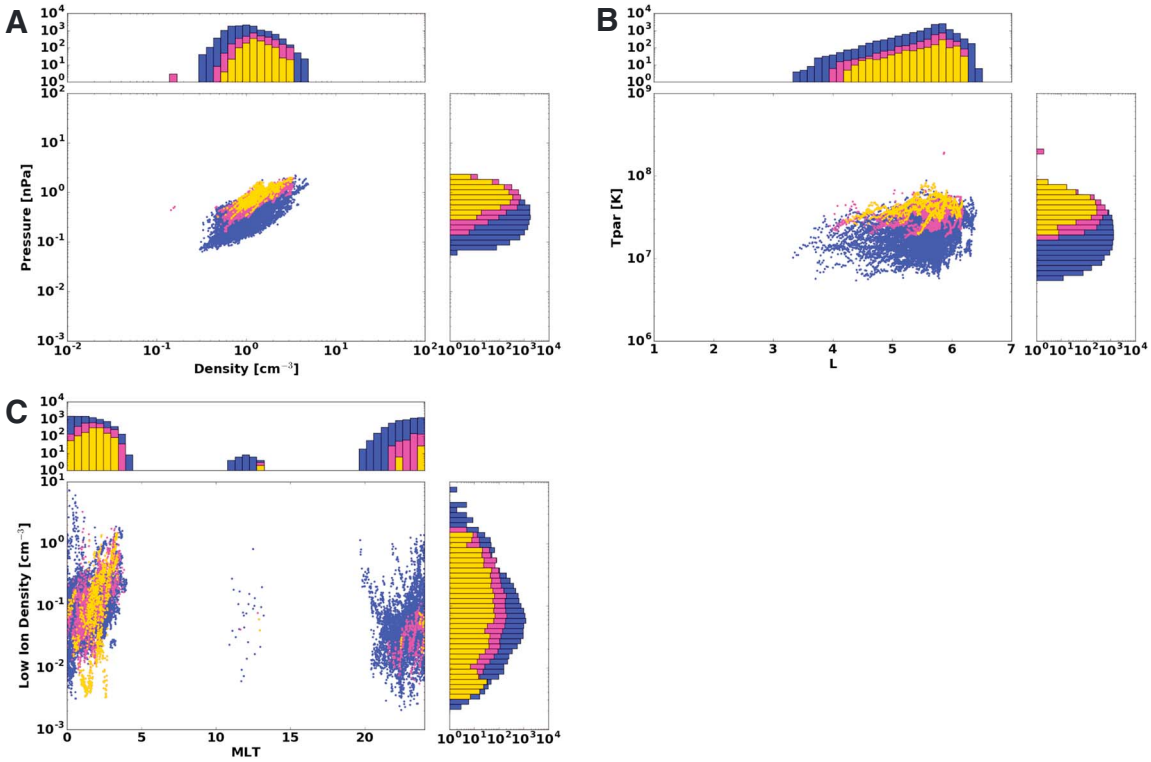

Figure 9. Resampled EFW spacecraft potential values, the HOPE instrument electron temperature (T_e), electron density (n_e), spacecraft potential corrected low-energy ion density (n_i), electron pressure (p_e), and the ephemeris MLT and L parameters from February 2013 to June 2013 at times where the 3 keV electron energy flux is above 3×10^7 keV cm^{-2} s^{-1} sr^{-1} keV^{-1}. (a) n_e compared to p_e. (b) L compared to T_e. (c) Low-energy ion density compared to MLT. The gold represents charging less than −25 V, the magenta represents charging less than −1 V, and blue represents charging above −1 V. The side panels represent the number of points contained within each interval.

Figure 8 examines spacecraft charging as a function of combinations of these variables. We only use EFW data here because we wanted to include times with little or no spacecraft charging (above −10 V), which the HOPE algorithm cannot detect. The color of each point represents the degree of spacecraft charging during the measurement, with gold indicating −25 V or lower potential, magenta <−1 V, and blue >−1 V. Figure 8a shows the hot (>200 eV) HOPE partial electron density compared with electron pressure. Times of spacecraft charging tended to occur with electron number densities above 1 cm^{-3} and electron pressure above 0.1 nPa. However, high electron densities and electron pressure do not necessarily indicate that there will be negative spacecraft charging, as there are many noncharging times that have the same density and pressure.

Figure 8b shows L and electron temperature. We see that times of spacecraft charging tended to occur above $L = 5$ and with electron temperatures above 4×10^7 K, or 3.45 keV. However, once again, high L and high electron temperature do not necessarily mean there will be charging. Figure 8c displays MLT and the spacecraft potential corrected low-energy ion density using the HOPE instrument protons between 1 and 210 eV. The method we used to describe spacecraft potential correction in the low-energy ion densities can be found in L. K. Sarno-Smith et al. (Local time variations of high-energy plasmaspheric ion pitch angle distributions, submitted to *Journal of Geophysical Research: Space Physics*). We see that the most intense charging events involved extremely low-energy ion densities, which is what we would expect because the ions are accelerated. As noted before, some caution must be taken in using this result, however, since charging accelerated low-energy ions to higher energies and make it "appear" like there was no low-energy ion population. Most intense and moderate charging events occurred in the postmidnight sector between $0 < \text{MLT} < 5$, with a few events also occurring in the premidnight sector.

Figure 8 demonstrates that electron pressure is more of a controlling factor in intense charging events than any of the other variables. Since pressure is constructed from electron temperature and density ($p_e = n_e k_B T_e$, where k_B is Boltzmann's constant), we can state that in addition to high electron temperatures, high electron densities must be present in order to have surface charging on the Van Allen Probes. This is expected since

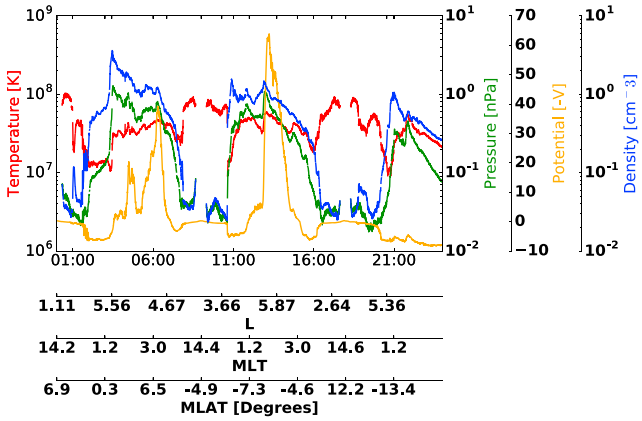

Figure 10. An example of negative spacecraft potential (orange) from EFW connected to the HOPE instrument electron temperature (red), electron pressure (green), and 30 eV and above electron number density (blue) on 14 February 2013 from Van Allen Probes A. The satellite was not in eclipse on this day.

once a certain threshold current from the electron density on the spacecraft is reached, photoelectron emission current is superseded as the dominant current on the spacecraft surface and the potential runs negative. The amount of negative spacecraft charge is determined by the potential necessary to drive the electron fluxes away from the spacecraft body and restore current balance. The potential is comparable to the electron temperature, so it makes sense that high pressure is a controlling factor in intense charging events. However, high electron densities and temperatures do not necessarily result in negative charging. Also, more intense charging events were related to higher electron pressure, suggesting that pressure may be a controlling factor in the intensity of a charging event, perhaps more than temperature.

Figure 9 shows the same variables described above at times when the 3 eV electron energy flux is above 3×10^7 keV cm^{-2} s^{-1} sr^{-1} keV^{-1}. Identical to Figure 8, gold is <−25 V, magenta is <−1 V and blue is all other times from February 2013 to June 2013. We find similar results as Figure 8, where electron pressure in panel A seems to be the largest controlling factor in determining if an event will charge negatively. Once again, however, the satellite can measure high electron pressure and high keV electron fluxes, but not show any indication of spacecraft charging in the EFW data set. Most notable about Figure 9 is that by excluding times

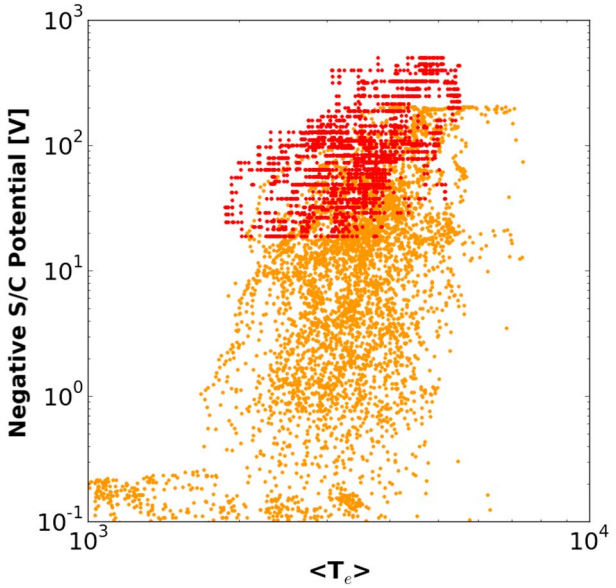

Figure 11. Van Allen Probes satellite A average electron temperatures compared to EFW (orange) and HOPE (red) negative spacecraft potentials from February 2013 to June 2013. Average electron temperature is in eV.

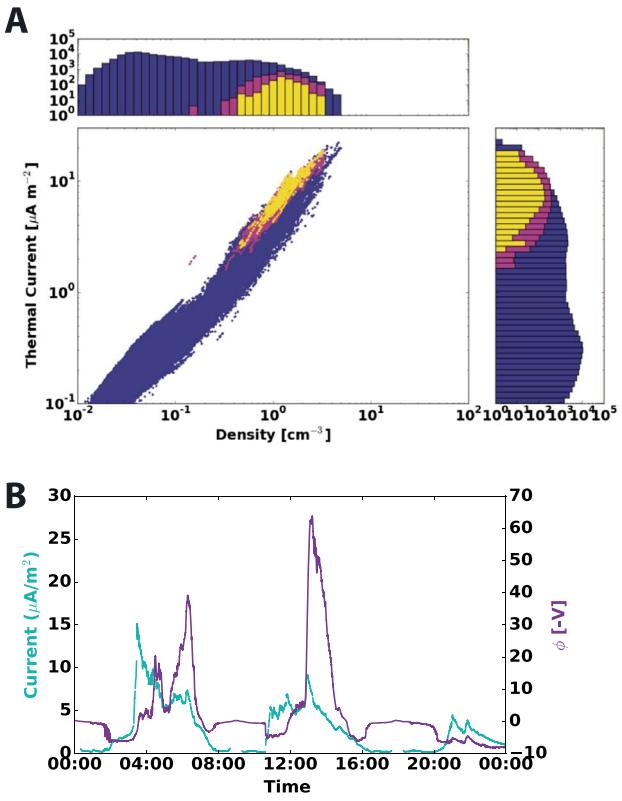

Figure 12. (a) The calculated spacecraft thermal electron current (μA m^{-2}) compared to electron pressure from February 2013 to June 2013. The gold represents charging less than −25 V, the magenta represents charging less than −1 V, and blue represents charging above −1 V. The side panels represent the number of points contained within each interval. (b) A case study from Van Allen Probes A of thermal electron current (aqua) compared with negative spacecraft potential (purple), on 14 February 2013. The satellite was not in eclipse on this day.

where the electron energy flux is below 3×10^7 keV cm^{-2} s^{-1} sr^{-1} keV^{-1}, many of the noncharging blue points are removed from these plots. Thus, once electron keV energy flux is high, then charging may occur depending on additional unknown circumstances.

The case study shown in Figure 10 highlights the relationship between electron density, electron pressure, and temperature with spacecraft potential. We see in the first charging event at 4:00 UT through 7:00 UT on 14 February 2013 on Van Allen Probes A that there was very high density and pressure along with steadily increasing electron temperature during this period. There was a dip in electron pressure at 5:30 UT corresponding with a spacecraft potential drop again to approximately 0 V. Another rise in spacecraft potential occurred at 6:00 UT as electron pressure rose again.

The second spacecraft charging event in Figure 10 occurred at 13:30 UT as temperature suddenly spiked in conjunction with a rapid rise in electron density. These three parameters then slowly decreased over the next hour, restoring spacecraft potential to approximately 0 V. In the afternoon, between 16:00 UT and 21:00 UT, we see that electron temperatures were very high, but the electron pressure remained low because the electron density was low. There was no significant charging during this later interval. The magnitude of electron temperature, number density, and pressure does not determine the intensity of the spacecraft charging event.

Figure 11 shows Van Allen Probes A average electron temperature compared to the negative spacecraft potential from EFW and HOPE between February 2013 and June 2013. Average temperature is calculated using an approximation from *Thomsen et al.* [2013]:

$$< T_e > = \frac{(n_i \times 5) + (n_e T_e)}{n_i + n_e}, \quad (2)$$

where $< T_e >$ is the average electron temperature, n_i is the low-energy ion density from 1 to 200 eV, n_e is the hot electron density calculated from HOPE differential number electron fluxes above 200 eV, and T_e is the hot electron temperature in eV above 200 eV. The approximation is used because there is backscatter contamination in the low-energy electrons, so assuming quasineutrality, the measured low-energy ion density serves as a more reliable electron density measurement. The factor of 5 is an approximation for the low-energy ion temperature of 5 eV. *Thomsen et al.* [2013] had found $< T_e >$ determined the intensity of the spacecraft potential. We do not find a strong or as clear a result here; however, we do see that spacecraft potential tends to rise with increasing temperature above a threshold average electron temperature of 2000 K.

Another factor to consider is the thermal electron current compared to the photoemission current. Negative spacecraft charging occurs when the magnitude of the thermal electron currents generated from elevated high energy electron fluxes exceed the photoemission current. Figure 12 shows the thermal electron

current versus electron pressure and a case study of Van Allen Probes A thermal electron current compared to spacecraft charging on 8 February 2013. Thermal electron current is calculated as

$$I_{\text{therm}} = \beta n \sqrt{T_e}, \tag{3}$$

where β is a constant of 0.094 that emerges from unit conversion, n is the electron number density above 200 eV in cm^{-3}, and T_e is the electron temperature. The number density and electron temperature were calculated from electron differential number fluxes above 200 eV. Figure 12a shows a statistical study of thermal electron current. Higher thermal electron currents are associated with more intense negative charging, but high thermal electron currents also occur during times of no spacecraft charging. Figure 12 shows the thermal electron current from the same day as in Figure 10. The highest thermal electron current occurs during the first and less intense charging event on 14 February 2013. However, the thermal electron currents are still high in the second and more intense event. When the position of insulators on the spacecraft is taken into consideration, the thermal electron current difference between the conducting portion of the spacecraft and insulated portions may cause the satellite to charge more negatively at some times [*Davis et al.*, 2012].

6. Conclusions

In this study, spacecraft charging on a conducting spacecraft within geosynchronous orbit was explored. Unlike previous nonconducting satellite missions, spacecraft charging on the conducting Van Allen Probes was not as intense. The Van Allen Probes tended to charge slightly positive; however, times of significant negative charging still occurred in the time period we examined.

We explored statistics based on the distribution of spacecraft charging measured by EFW and its relationship with MLT and L. It was found that most slightly negative charging occurred at low Ls, at daytime MLTs, and in Earth's shadow. Positive charging occurred at all Ls and MLTs. Strong positive charging occurred across the nightside at high Ls, while strong negative charging occurred primarily at high Ls in the postmidnight sector. This strong negative charging above $L > 3$ occurred, while the spacecraft was not in eclipse. We think the strong positive charging is due to bad data; however, we do not have an explanation of why it is mostly centered around midnight and in the premidnight sector.

To obtain spacecraft charging values below the −200 V limit of EFW, we also developed an algorithm to determine the level of spacecraft charging by extracting the charging line seen in the HOPE instrument H^+ spectra. From this technique, we found that EFW underestimated spacecraft charging by approximately 5 V or 17%. During times when the spacecraft charge reached below −50 V, the two methods provided very similar measurements. However, the charging line extraction method was not a stand alone method, so we concluded that it was best to use both the EFW spacecraft potential measurements and the charging line extraction method to obtain the best understanding of spacecraft charging in the Van Allen Probes.

The connection between keV electron energy fluxes and spacecraft charging was presented in this study. Similar to previous results, we found that for the Van Allen Probes there was a connection between spacecraft charging and keV electron energy fluxes. The connection between high energy fluxes during charging times extended from 1 eV to 5 keV. This study did find an electron energy flux threshold of 3×10^7 keV cm^{-2} s^{-1} sr^{-1} keV^{-1} for 3 keV electrons where intense charging is more likely to occur if this threshold is met; however, there are times the electron energy fluxes reach this threshold and significant negative spacecraft charging does not occur.

Spacecraft charging was compared with electron temperature, pressure, electron density, low-energy (1–210 eV) H^+ density, MLT, and L. In times of charging on the Van Allen Probes, electron temperature, electron density, and, consequently, electron pressure were all generally elevated during times of significant charging. The strongest connection was between electron pressure and spacecraft charging. However, high electron pressure did not always correlate with times of negative spacecraft charging, so further exploration of this connection is necessary. *Thomsen et al.* [2013] had found that the intensity of a spacecraft charging event was determined by average electron temperature, but we did not find as strong of a relationship in our study with the Van Allen Probes.

Our results built upon previous work, and we have shown for a conducting spacecraft that there is a keV electron energy flux threshold that once surpassed, increases the likelihood of charging to occur. Future work is necessary to determine exactly what combination of parameters results in intense negative charging on the

Van Allen Probes or another similar conducting spacecraft. The extreme care to maximize conductivity on the Van Allen Probes has resulted in a spacecraft that charged negatively infrequently, allowing for low-energy ion measurement with greater certainty and reduced arcing potential on the Van Allen Probes.

Acknowledgments
The University of Michigan co-authors would like to thank the University of Michigan Rackham Graduate school, NASA, and the NSF for sponsoring this work under grants NWX11AO60G, NWX144AC02G, and AGS-1102863. Work at Los Alamos National Laboratory was performed under the auspices of the U.S. Department of Energy, LA-UR-15-27864. This work was supported by Van Allen Probes-ECT funding provided by JHU/APL contract 967399 under NASA's Prime contract NAS5-01072. Data used to generate figures for this project came from the Van Allen Probes data center at http://www.vanallenprobes-ect.lanl.gov/data_pub/. We would also like to thank Brian Walsh for his useful science direction.

References

Choi, H.-S., J. Lee, K.-S. Cho, Y.-S. Kwak, I.-H. Cho, Y.-D. Park, Y.-H. Kim, D. N. Baker, G. D. Reeves, and D.-K. Lee (2011), Analysis of GEO spacecraft anomalies: Space weather relationships, *Space Weather*, *9*, S06001, doi:10.1029/2010SW000597.

Craven, P., R. Olsen, J. Fennell, D. Croley, and T. Aggson (1987), Potential modulation on the SCATHA spacecraft, *J. Spacecr. Rockets*, *24*(2), 150–157.

Davis, V., M. Mandell, N. Baker, M. Brown-Hayes, G. Davis, R. Maurer, and C. Herrmann (2012), Surface-charging analysis of the radiation belt storm probe and magnetospheric MultiScale spacecraft, *IEEE Trans. Plasma Sci.*, *40*(2), 262–273.

DeForest, S. E. (1972), Spacecraft charging at synchronous orbit, *J. Geophys. Res.*, *77*(4), 651–659.

DeForest, S. E. (1973), Electrostatic potentials developed by ATS-5, in *Photon and Particle Interactions with Surfaces in Space*, edited by R. J. L. Grard, pp. 263–267, Springer, Netherlands.

Funsten, H., et al. (2014), Helium, Oxygen, Proton, and Electron (HOPE) mass spectrometer for the Radiation Belt Storm Probes mission, in *The Van Allen Probes Mission*, pp. 423–484, Springer, Netherlands.

Garrett, H. B. (1981), The charging of spacecraft surfaces, *Rev. Geophys. Space Phys.*, *19*(4), 577–616.

Grard, R., K. Knott, and A. Pedersen (1983), Spacecraft charging effects, in *Progress in Solar-Terrestrial Physics*, edited by J. G. Roederer, pp. 289–304, Springer, Netherlands.

Harris, J. T. (2003), Spacecraft charging at geosynchronous altitudes: Current-balance and critical temperature in a non-Maxwellian plasma, *Tech. Rep., No. AFIT/GAP/ENP/03-05*, Air Force Inst. of Tech. Wright-Patterson AFB OH Sch. of Eng. and Manage.

Harvey, P., et al. (1995), The electric field instrument on the Polar satellite, *Space Sci. Rev.*, *71*(1–4), 583–596.

Johnson, C. Y., and E. B. Meadows (1955), First investigation of ambient positive-ion composition to 219 km by rocket-borne spectrometer, *J. Geophys. Res.*, *60*(2), 193–203.

Katz, I., V. Davis, and D. B. Snyder (1998), Mechanism for spacecraft charging initiated destruction of solar arrays in GEO, paper AIAA 1998–1002 presented at 36th AIAA Aerospace Sciences Meeting and Exhibit, Reno, Nevada, 12–15 Jan.

Kirby, K., et al. (2014), Radiation belt storm probes—Observatory and environments, in *The Van Allen Probes Mission*, edited by N. Fox and J. L. Burch, pp. 59–125, Springer, New York.

Koons, H., J. Mazur, A. Lopatin, D. Pitchford, A. Bogorad, and R. Herschitz (2006), Spatial and temporal correlation of spacecraft surface charging in geosynchronous orbit, *J. Spacecr. Rockets*, *43*(1), 178–185.

Laframboise, J., and M. Kamitsuma (1983), The threshold temperature effect in high-voltage spacecraft charging, *Tech. Rep.*, York Univ. Downsview, Ontario.

Lai, S. T., and D. J. Della-Rose (2001), Spacecraft charging at geosynchronous altitudes: New evidence of existence of critical temperature, *J. Spacecr. Rockets*, *38*(6), 922–928.

Lai, S. T., and M. Tautz (2006), High-level spacecraft charging in eclipse at geosynchronous altitudes: A statistical study, *J. Geophys. Res.*, *111*, A09201, doi:10.1029/2004JA010733.

Lanzerotti, L., C. Breglia, D. Maurer, G. Johnson, and C. Maclennan (1998), Studies of spacecraft charging on a geosynchronous telecommunications satellite, *Adv. Space Res.*, *22*(1), 79–82.

Lanzerotti, L. J. (2001), Space weather effects on communications, in *Space Storms and Space Weather Hazards*, edited by I. A. Daglis, pp. 313–334, Springer, Netherlands.

Mauk, B., N. Fox, S. Kanekal, R. Kessel, D. Sibeck, and A. Ukhorskiy (2014), Science objectives and rationale for the radiation belt storm probes mission, in *The Van Allen Probes Mission*, edited by N. Fox and J. L. Burch, pp. 3–27, Springer, New York.

Mazur, J. E., and T. P. O'Brien (2012), Comment on "Analysis of GEO spacecraft anomalies: Space weather relationships" by Ho-Sung Choi et al., *Space Weather*, *10*, S03003, doi:10.1029/2011SW000738.

Mullen, E. G., M. S. Gussenhoven, D. A. Hardy, T. A. Aggson, B. G. Ledley, and E. Whipple (1986), SCATHA survey of high-level spacecraft charging in sunlight, *J. Geophys. Res.*, *91*(A2), 1474–1490, doi:10.1029/JA091iA02p01474.

Olsen, R. C. (1981), Modification of spacecraft potentials by thermal electron emission on ATS-5, *J. Spacecr. Rockets*, *18*(6), 527–532.

Olsen, R. C. (1983), A threshold effect for spacecraft charging, *J. Geophys. Res.*, *88*(A1), 493–499.

Olson, W., and K. Pfitzer (1977), Magnetospheric magnetic field modeling, *Annu. Sci. Rep. F44620-75-C-0033*, McDonnell Douglas Astronautics, Huntington Beach, Calif.

Reagan, J., R. Nightingale, E. Gaines, R. Meyerott, and W. Imhof (1981), *Role of Energetic Particles in Charging/Discharging of Spacecraft Dielectrics*, NASA. Lewis Res. Cent. Spacecr. Charging Technol., pp. 74–85 pp., Palo Alto, Calif.

Reasoner, D., C. Chappell, and W. Lennartsson (1976), Relationship between ATS-6 spacecraft-charging occurrences and warm plasma encounters, paper presented at Symposium on Spacecraft Charging by Magnetospheric Plasmas, pp. 89–101, Washington, D. C., 16–19 Jun.

Rosen, A. (1976), Spacecraft charging by magnetospheric plasmas, *IEEE Trans. Nucl. Sci.*, *23*(6), 1762–1768.

Rubin, A., H. B. Garrett, and A. Wendel (1980), Spacecraft charging on ATS-5, *Tech. Rep., No. AFGL-TR-80-0168*, Air Force Geophys. Lab., Hanscom AFB, Bedford, Mass.

Sarno-Smith, L. K., M. W. Liemohn, R. M. Katus, R. M. Skoug, B. A. Larsen, M. F. Thomsen, J. R. Wygant, and M. B. Moldwin (2015), Postmidnight depletion of the high-energy tail of the quiet plasmasphere, *J. Geophys. Res. Space Physics*, *120*, 1646–1660, doi:10.1002/2014JA020682.

Thomsen, M. F., M. G. Henderson, and V. K. Jordanova (2013), Statistical properties of the surface-charging environment at geosynchronous orbit, *Space Weather*, *11*, 237–244, doi:10.1002/swe.20049.

Wygant, J., et al. (2014), The electric field and waves instruments on the radiation belt storm probes mission, in *The Van Allen Probes Mission*, edited by N. Fox and J. L. Burch, pp. 183–220, Springer, New York.